Collective phase oscillation in two-dimensional *d*-wave superconductors

Y. Ohashi and S. Takada
Institute of Physics, University of Tsukuba, Ibaraki 305, Japan
(Received 20 August 1999; revised manuscript received 13 March 2000)

We theoretically investigate the Carlson-Goldman (CG) mode in two-dimensional $d_{x^2-y^2}$-wave superconductivity. In conventional *s*-wave superconductors, it is known that the CG mode is observed as a peak in the structure function of the pair field susceptibility $S(\mathbf{q},\omega)$ only just below the transition temperature T_c and only in dirty systems. On the other hand, in the *d*-wave state, we show that the peak structure can be observed down to $T \simeq 0.2T_c$ in clean systems. Furthermore, we also show that the peak splits into two when the direction of the momentum $\mathbf{q}$ deviates from the q_x or q_y axes, or nodal directions of the order parameter. These features originate from a singularity in the charge-density fluctuation due to the presence of the nodes of the *d*-wave order parameter: It enhances the screening of the long-range Coulomb interaction so that the CG mode can exist far below T_c. We also investigate a quasi-two-dimensional system, and show that the Josephson plasma can be observed in $S(\mathbf{q},\omega)$ when $\mathbf{q}$ is parallel to the *c* direction.

I. INTRODUCTION

The Goldstone mode which accompanies the spontaneous gauge-symmetry breaking is one of the most fundamental phenomena in superconductivity. In neutral systems, it is known as the Anderson-Bogoliubov mode (phason).[1] In charged systems, it is the Carlson-Goldman (CG) mode.[2,3] Both modes have linear dispersions, and they are the collective phase oscillations of the superconducting order parameter. In the language of the two-fluid picture, they are the oscillations of the superfluid component.

Besides the superfluid component, the quasiparticles which are excited thermally are also crucial, particularly for the CG mode. For conventional (isotropic) *s*-wave superconductors, the following important roles have been clarified:

(i) Screening effect: In charged superconductors, the Goldstone mode does not exist at $T=0$ because of the long-range Coulomb interaction between electrons (Anderson-Higgs mechanism).[4] In order for the CG mode to appear, the Coulomb interaction between superfluid carriers must be screened out by the quasiparticles. Thus the CG mode appears only just below the transition temperature (T_c) where a large number of quasiparticles are excited thermally.[2,3,5–14]

(ii) Landau damping: The CG mode is observed as a peak in the structure function of the pair field susceptibility $S(\mathbf{q},\omega)$; it is experimentally measured by a tunneling experiment under a magnetic field.[15–18] Since the quasiparticles cause the Landau damping which makes the CG mode overdamped, the suppression of the damping effect is needed in observing the CG mode. In clean superconductors, the Landau damping is so strong that the peak does not appear in $S(\mathbf{q},\omega)$,[14] even if the Coulomb interaction is screened out. It is observed only in dirty systems, because the Landau damping is suppressed by potential scatterings.[5–8,11,12,14]

Since the discovery of high-T_c cuprates, the $d_{x^2-y^2}$-wave superconductivity has attracted much attention.[19] In this state, since a large number of the quasiparticles can be excited thermally around the nodes of the *d*-wave order parameter, the Landau damping should be stronger than that in the conventional *s*-wave one. Furthermore, when we introduce potential scatterings in order to suppress the damping, the depairing effect by the scatterings increases the quasiparticles in the *d*-wave state, which may cause the Landau damping. Thus, when only the smearing effect on the CG mode is considered, observation of this collective mode seems more difficult in the *d*-wave state than in the *s*-wave one.

However, in addition to the stronger Landau damping, we can also expect a stronger screening effect by the quasiparticles around the nodes in the *d*-wave state. Then if the CG mode can survive by the screening effect down to the low-temperature region where the Landau damping is weak, it may be observed as a peak in $S(\mathbf{q},\omega)$ overwhelming the Landau damping. Thus it is a crucial problem whether the nodes work positively or negatively for the CG mode at low temperatures. At the present stage, within a pole analysis, it is reported that the CG mode is overdamped near T_c in the *d*-wave state even in the presence of the potential scatterings.[20] However, the CG mode at low temperatures has not been investigated yet.

In this paper, we present a microscopic theory for the CG mode in two-dimensional *d*-wave superconductors in order to clarify nodal effects on this mode. We assume a circular Fermi surface, and calculate $S(\mathbf{q},\omega)$ within the random phase approximation (RPA) in terms of the pairing and the long-range Coulomb interactions. Nonmagnetic impurity scatterings are taken into account within the *t*-matrix approximation. We also consider a quasi-two-dimensional system, and investigate $S(\mathbf{q},\omega)$ in the case when the momentum $\mathbf{q}$ is parallel to the *c* axis.

This paper is organized as follows: We present our formulation in Sec. II. We investigate the CG mode in clean systems and dirty ones, respectively, in Secs. III and IV. We extend our theory to a quasi-two-dimensional system in Sec. V, which is followed by the summary in Sec. VI. Throughout this paper, the clean system means the one in which potential scatterings are absent. When the potential scatterings is present, the system is called the dirty one.

II. FORMULATION

A. Model two-dimensional *d*-wave superconductor

We investigate the two-dimensional *d*-wave superconductivity which is described by the Hamiltonian[13,14,21]

$$H=\sum_{\mathbf{p}} \Psi_{\mathbf{p}}^{\dagger}(\xi_{\mathbf{p}}\tau_3-\Delta_{\mathbf{p}}\tau_1)\Psi_{\mathbf{p}} + \frac{1}{2}\sum_{\mathbf{q}}\left[V(\mathbf{q})\rho_{3\mathbf{q}}\rho_{3-\mathbf{q}} - \frac{g}{2}(\rho_{1\mathbf{q}}\rho_{1-\mathbf{q}}+\rho_{2\mathbf{q}}\rho_{2-\mathbf{q}})\right]+H_{\mathrm{imp}}, \tag{2.1}$$

where $\Psi_{\mathbf{p}}^{\dagger}=(c_{\mathbf{p}\uparrow}^{\dagger}, c_{-\mathbf{p}\downarrow})$ is the Nambu field operator in which $c_{\mathbf{p}\sigma}^{\dagger}$ is an electron creation operator with spin σ; $\tau_i (i=1,2,3)$ is the Pauli matrix. The kinetic energy is given by $\xi_{\mathbf{p}}=p^2/(2m)-\varepsilon_{\mathrm{F}}$ $(p^2=p_x^2+p_y^2)$ with ε_{F} being the Fermi energy.

We put the long-range Coulomb interaction $V(\mathbf{q})=4\pi e^2/q^2$ assuming a three-dimensional material with the two-dimensional electronic band $\xi_{\mathbf{p}}$.[22] As for the pairing interaction, we assume the separable interaction $H_{\mathrm{pair}}=-g\Sigma_{\mathbf{p},\mathbf{p}'}\gamma_{\mathbf{p}}\gamma_{\mathbf{p}'}c_{\mathbf{p}\uparrow}^{\dagger}c_{-\mathbf{p}\downarrow}^{\dagger}c_{-\mathbf{p}'\downarrow}c_{\mathbf{p}'\uparrow}$, where $\gamma_{\mathbf{p}}=\sqrt{2}\cos(2\theta_{\mathbf{p}})$ is the basis function of the $d_{x^2-y^2}$-wave superconductivity; $\theta_{\mathbf{p}}$ is the polar angle of $\mathbf{p}$ around the p_z axis measured from the p_x axis. In this case, the order parameter has the form $\Delta_{\mathbf{p}}=\gamma_{\mathbf{p}}\Delta$. We have chosen $\Delta_{\mathbf{p}}$ being real and proportional to the τ_1-component in Eq. (2.1).

In Eq. (2.1), $\rho_{i\mathbf{q}}=\Sigma_{\mathbf{p}}\gamma_{\mathbf{p}-\mathbf{q}/2}^{i}\Psi_{\mathbf{p}-\mathbf{q}}^{\dagger}\tau_i\Psi_{\mathbf{p}}$ $(i=1,2,3)$, where $\gamma_{\mathbf{p}}^{i}=(\gamma_{\mathbf{p}}^{1},\gamma_{\mathbf{p}}^{2},\gamma_{\mathbf{p}}^{3})\equiv(\gamma_{\mathbf{p}},\gamma_{\mathbf{p}},1)$. Physically, $\rho_{3\mathbf{q}}$ is the charge-density operator, while $\rho_{1\mathbf{q}}$ and $\rho_{2\mathbf{q}}$ describe, respectively, the amplitude and phase fluctuation of the order parameter.

The last term in Eq. (2.1) represents the nonmagnetic impurity scatterings:

$$H_{\mathrm{imp}}=u\sum_{\mathbf{R}_i,\mathbf{p},\mathbf{p}'} e^{-i(\mathbf{q}-\mathbf{q}')\cdot\mathbf{R}_i}\Psi_{\mathbf{p}}^{\dagger}\tau_3\Psi_{\mathbf{p}'}, \tag{2.2}$$

where u is an impurity potential at $\mathbf{R}_i$. For simplicity, we have assumed the s-wave scattering in Eq. (2.2).

B. Structure function of pair field susceptibility

The structure function of the pair field susceptibility $S(\mathbf{q},\omega)$ is given by

$$S(\mathbf{q},\omega)=\frac{1}{\omega}\mathrm{Im}[\Pi_{22}(\mathbf{q},\omega)], \tag{2.3}$$

where $\Pi_{22}(\mathbf{q},\omega)$ is the correlation function of the phase fluctuation of the order parameter:

$$\Pi_{ij}(\mathbf{q},\omega)=-i\int_0^{\infty}dt e^{i\omega t}\langle[\rho_{i\mathbf{q}}(t),\rho_{j-\mathbf{q}}(0)]\rangle \quad (i,j=1,2,3). \tag{2.4}$$

Equation (2.4) also defines the charge-density fluctuation Π_{33}, the amplitude fluctuation Π_{11} and the coupling of different kinds of fluctuations $\Pi_{ij:i\neq j}$.

In calculating Π_{22}, it is convenient to introduce the following polarization function in the Matsubara formalism

$$\Pi_{ij}(\mathbf{q},i\nu_n)=-\int_0^{\beta}d\tau e^{i\nu_n\tau}\langle T_{\tau}\{\rho_{i\mathbf{q}}(\tau)\rho_{j-\mathbf{q}}(0)\}\rangle, \tag{2.5}$$

and the thermal one-particle Green's function

$$G(\mathbf{p},i\omega_m)=\frac{1}{i\omega_m-\xi_{\mathbf{p}}\tau_3+\Delta_{\mathbf{p}}\tau_1}, \tag{2.6}$$

where $\beta=1/T$, while ν_n and ω_m express, respectively, the Boson and the Fermion Matsubara frequencies. $\Pi_{ij}(\mathbf{q},\omega)$ is related to $\Pi_{ij}(\mathbf{q},i\nu_n)$ as $\Pi_{ij}(\mathbf{q},\omega)=\Pi_{ij}(\mathbf{q},i\nu_n\rightarrow\omega_+\equiv\omega+i\delta)$.

1. Clean system

In the clean system, the lowest-order polarization functions in terms of the interactions are obtained as[13,14]

$$\Pi_{22}^{0}(\mathbf{q},\omega)=\sum_{\mathbf{p}}\gamma_{\mathbf{p}}^2\left(1-\frac{\xi_+\xi_-+\Delta_{\mathbf{p}}^2}{E_+E_-}\right)\times\frac{E_+-E_-}{(E_+-E_-)^2-\omega_+^2}[f(E_+)-f(E_-)] -\sum_{\mathbf{p}}\gamma_{\mathbf{p}}^2\left(1+\frac{\xi_+\xi_-+\Delta_{\mathbf{p}}^2}{E_+E_-}\right)\frac{E_++E_-}{(E_++E_-)^2-\omega_+^2}\times[1-f(E_+)-f(E_-)], \tag{2.7}$$

$$\Pi_{33}^{0}(\mathbf{q},\omega)=\sum_{\mathbf{p}}\left(1+\frac{\xi_+\xi_--\Delta_{\mathbf{p}}^2}{E_+E_-}\right)\frac{E_+-E_-}{(E_+-E_-)^2-\omega_+^2}\times[f(E_+)-f(E_-)] -\sum_{\mathbf{p}}\left(1-\frac{\xi_+\xi_--\Delta_{\mathbf{p}}^2}{E_+E_-}\right)\frac{E_++E_-}{(E_++E_-)^2-\omega_+^2}\times[1-f(E_+)-f(E_-)], \tag{2.8}$$

where f is the Fermi distribution function; $E_{\pm}=\sqrt{\xi_{\pm}^2+\Delta_{\mathbf{p}}^2}$, and $\xi_{\pm}=\xi_{\mathbf{p}}\pm\mathbf{v}_F\cdot\mathbf{q}/2$ ($\mathbf{v}_F$: Fermi velocity). In Eqs. (2.7) and (2.8), we have expanded $\xi_{\mathbf{p}\pm\mathbf{q}/2}$ up to $O(q)$ assuming $q\lesssim O(1/\xi)$ $(\xi=v_{\mathrm{F}}/T_{\mathrm{c}}$: superconducting coherence length).[13,14] We have also expanded $\Delta_{\mathbf{p}+\mathbf{q}/2}$ as $\Delta_{\mathbf{p}+\mathbf{q}/2}\simeq\Delta_{\mathbf{p}}\pm(\mathbf{q}/2)\cdot\nabla_{\mathbf{p}}\Delta_{\mathbf{p}}$, and have neglected the second term, because it is smaller than the first one by $O(\Delta/\varepsilon_{\mathrm{F}})$ for $q\lesssim O(1/\xi)$.[21,23]

Under these approximations for $\xi_{\mathbf{p}}$ and $\Delta_{\mathbf{p}}$, we find $\Pi_{12}^{0}(\mathbf{q},\omega)=\Pi_{21}^{0}(\mathbf{q},\omega)=\Pi_{13}^{0}(\mathbf{q},\omega)=\Pi_{31}^{0}(\mathbf{q},\omega)=0$.[10,13,14] Then, since the amplitude fluctuation does not couple with the charge-density fluctuation nor the phase fluctuation, we do not need Π_{11}^{0} in studying Π_{22}. On the other hand, the phase-charge coupling Π_{23}^{0} is finite as

$$\Pi_{23}^{0}(\mathbf{q},\omega)=-\Pi_{32}^{0}(\mathbf{q},\omega) =-i\omega_+\sum_{\mathbf{p}}\gamma_{\mathbf{p}}\frac{\Delta_{\mathbf{p}}}{E_+E_-}\frac{E_+-E_-}{(E_+-E_-)^2-\omega_+^2}\times[f(E_+)-f(E_-)] -i\omega_+\sum_{\mathbf{p}}\gamma_{\mathbf{p}}\frac{\Delta_{\mathbf{p}}}{E_+E_-}\frac{E_++E_-}{(E_++E_-)^2 i\omega_+^2}\times[1-f(E_+)-f(E_-)]. \tag{2.9}$$

Taking into account the interactions within RPA, we obtain[13,14]

$$\Pi_{22}(\mathbf{q},\omega)=\frac{\overline{\Pi}_{22}(\mathbf{q},\omega)}{1+(g/2)\overline{\Pi}_{22}(\mathbf{q},\omega)}, \tag{2.10}$$

where

$$\overline{\Pi}_{22}(\mathbf{q},\omega)=\Pi^0_{22}(\mathbf{q},\omega)+\Pi^0_{23}(\mathbf{q},\omega)\frac{V(\mathbf{q})}{1-V(\mathbf{q})\Pi^0_{33}(\mathbf{q},\omega)}\times\Pi^0_{32}(\mathbf{q},\omega). \tag{2.11}$$

The gap equation can be written with Π^0_{22} as[13,14]

$$1+\frac{g}{2}\Pi^0_{22}(0,0)=0. \tag{2.12}$$

The CG mode is obtained as a pole of $\Pi_{22}(\mathbf{q},\omega)$. From Eqs. (2.10) and (2.12), the equation of the CG mode is $\overline{\Pi}_{22}(\mathbf{q},\omega)-\Pi^0_{22}(0,0)=0$. In this paper, however, we solve the real part of this equation[13,14] when we calculate the dispersion and the velocity of the CG mode; this treatment neglects the damping of the CG mode. We consider the damping by examining how the mode appears as a peak in the spectrum of $S(\mathbf{q},\omega)$.

In numerical calculations, we transform the $\mathbf{p}$ summation in Π^0_{ij} into the ξ and angular integrations. Then the Coulomb interaction always appears as $V(\mathbf{q})N(0)(\equiv\overline{V})$ in Eq. (2.11), where $N(0)=m/(2\pi)$ is the density of states (DOS) at the Fermi level. We write $\overline{V}$ with use of the plasma energy $\omega_p=\sqrt{4\pi ne^2/m}$ (n: carrier density) as $\overline{V}=(\omega_p/T^0_c)^2/(q\xi_0)^2$, where $\xi_0=v_F/T^0_c$ with T^0_c being the transition temperature in the clean system, and put $\omega_p=10^4T^0_c\gg\Delta$. Although we do not show the ω_p dependence of our results explicitly, they are almost ω_p independent as far as $\omega_p\gg\Delta$.

2. Dirty system

(a) *Renormalized Matsubara frequency and gap equation.* We calculate the nonmagnetic impurity scatterings within the t-matrix approximation. The renormalized one-particle Green's function is then given by Eq. (2.6) with $i\omega_m$ being replaced by[24–28]

$$i\tilde{\omega}_m=i\omega_m+\gamma\frac{\Lambda(i\omega_m)}{C^2-\Lambda(i\omega_m)^2}, \tag{2.13}$$

where

$$\Lambda(i\omega_m)=\left\langle\frac{i\tilde{\omega}_m}{\sqrt{\tilde{\omega}_m^2+\Delta^2_{\mathbf{p}}}}\right\rangle_F. \tag{2.14}$$

Here, $\gamma=n_i/(\pi N(0))$, $C=1/(\pi uN(0))$, and n_i is the number density of the impurities; $\langle\cdots\rangle_F$ represents the average of $\mathbf{p}$ over the Fermi surface. Although our theory can treat arbitrary scattering strength, as typical cases we consider (i) the Born scattering ($C\gg1$), and (ii) the unitarity limit ($C=0$). Equation (2.13) is solved together with the gap equation

$$\ln\frac{T}{T^0_c}=\frac{2\pi}{\beta}\sum_{m\geqslant0}\left[\left\langle\frac{\gamma^2_{\mathbf{p}}}{\sqrt{\tilde{\omega}_m^2+\Delta^2_{\mathbf{p}}}}\right\rangle_F-\frac{1}{\omega_m}\right]. \tag{2.15}$$

(b) $\Pi_{22}(\mathbf{q},\omega)$ *in dirty system.* In the dirty system, Π^0_{ij} in Eq. (2.11) is replaced by Π^Γ_{ij} which is given by

$$\begin{pmatrix}\Pi^\Gamma_{22}&\Pi^\Gamma_{23}\\ \Pi^\Gamma_{32}&\Pi^\Gamma_{33}\end{pmatrix}=\begin{pmatrix}0&0\\0&\Pi^{\Gamma N}_{33}\end{pmatrix}+\frac{N(0)}{\pi i}\int_{-\infty}^{\infty}d\omega'\tanh\frac{\beta\omega'}{2}\times[\Xi_+(\mathbf{q},\omega,\omega')-\Xi_-(\mathbf{q},\omega,\omega')]. \tag{2.16}$$

(The derivation of Π^Γ_{ij} is explained in Appendix A.) Here $\Pi^{\Gamma N}_{33}$ represents Π^Γ_{33} in the normal state:

$$\Pi^{\Gamma N}_{33}(\mathbf{q},\omega)=-2N(0)\left[1-\frac{\omega}{\sqrt{(\omega+i\Gamma)^2-(v_Fq)^2}-i\Gamma}\right], \tag{2.17}$$

where $\Gamma=2\gamma/(1+C^2)$ is the damping rate of electrons. The matrix $\Xi_\pm(\mathbf{q},\omega,\omega')$ in Eq. (2.16) is given by

$$\Xi_\pm(\mathbf{q},\omega,\omega')=\hat{A}_\pm(\mathbf{q},\omega,\omega')-\overline{A}_\pm(\mathbf{q},\omega,\omega')\times\frac{1}{1+\alpha_\pm(\omega,\omega')A_\pm(\mathbf{q},\omega,\omega')}\times\alpha_\pm(\omega,\omega')\tilde{A}_\pm(\mathbf{q},\omega,\omega'). \tag{2.18}$$

We write the matrix elements of $A_\pm$, $\hat{A}_\pm$, $\overline{A}_\pm$, and $\tilde{A}_\pm$ as, for example,

$$A_\pm=\begin{pmatrix}A^{22}_\pm&A^{23}_\pm\\A^{32}_\pm&A^{33}_\pm\end{pmatrix}. \tag{2.19}$$

Then their matrix elements are given by

$$\begin{cases}A^{ij}_\pm(\mathbf{q},\omega,\omega')=\langle W^{ij}_\pm(\mathbf{p},\mathbf{q},\omega,\omega')\rangle_F,\\ \hat{A}^{ij}_\pm(\mathbf{q},\omega,\omega')=\langle\gamma^i_{\mathbf{p}}W^{ij}_\pm(\mathbf{p},\mathbf{q},\omega,\omega')\gamma^j_{\mathbf{p}}\rangle_F,\\ \overline{A}^{ij}_\pm(\mathbf{q},\omega,\omega')=\langle\gamma^i_{\mathbf{p}}W^{ij}_\pm(\mathbf{p},\mathbf{q},\omega,\omega')\rangle_F,\\ \tilde{A}^{ij}_\pm(\mathbf{q},\omega,\omega')=\langle W^{ij}_\pm(\mathbf{p},\mathbf{q},\omega,\omega')\gamma^j_{\mathbf{p}}\rangle_F.\end{cases} \tag{2.20}$$

The definition of $W^{ij}_\pm$ is as follows:

$$\begin{pmatrix}W^{22}_\pm&W^{23}_\pm\\W^{32}_\pm&W^{33}_\pm\end{pmatrix}=\pi i\frac{\sqrt{Z(\omega'_++\omega)^2-\Delta^2_{\mathbf{p}}}\pm\sqrt{Z(\omega'_\pm)^2-\Delta^2_{\mathbf{p}}}}{\eta^2-[\sqrt{Z(\omega'_++\omega)^2-\Delta^2_{\mathbf{p}}}\pm\sqrt{Z(\omega'_\pm)^2-\Delta^2_{\mathbf{p}}}]^2}\times\left[\tau_3\pm\frac{Z(\omega'_++\omega)Z(\omega'_\pm)-\Delta^2_{\mathbf{p}}+[Z(\omega'_++\omega)-Z(\omega'_\pm)]\Delta_{\mathbf{p}}\tau_2}{\sqrt{Z(\omega'_++\omega)^2-\Delta^2_{\mathbf{p}}}\sqrt{Z(\omega'_\pm)^2-\Delta^2_{\mathbf{p}}}}\right], \tag{2.21}$$

where $\eta=(\mathbf{p}_F/m)\cdot\mathbf{q}$, and $Z(\omega_\pm)$ is the renormalized frequency in Eq. (2.13) in which the analytic continuation, $i\nu_n\rightarrow\omega_\pm$, is taken. In Eq. (2.18), $\alpha_\pm(\omega,\omega')$ is defined by

$$\alpha_\pm(\omega,\omega')=\frac{\Gamma}{2\pi}\times\begin{cases}\tau_3 & \text{(Born)},\\ \dfrac{-1}{\Lambda(i\omega_m\rightarrow\omega'_+ +\omega)\Lambda(i\omega_m\rightarrow\omega'_\pm)} & \text{(unitarity)}.\end{cases}\tag{2.22}$$

III. COLLECTIVE PHASE OSCILLATION IN CLEAN SYSTEM

A. Dispersion

Figure 1 shows the dispersion of the CG mode at $\theta_\mathbf{q}=0$. ($\theta_\mathbf{q}$: polar angle of the momentum of the CG mode measured from the q_x axis.) The CG mode has a linear dispersion for small momenta as the phason in the neutral system. When temperature is lowered, the dispersion of the CG mode disappears from the high-energy region and disappears completely below $T\simeq 0.45T_c^0$. This is because the screening of the Coulomb interaction by quasiparticles is weaker at lower temperatures.

In neutral *d*-wave superconductivity, on the other hand, the phason exists down to $T=0$. In particular, at $T=0$ we obtain $\omega=(v_F/\sqrt{2})\cdot q$ for small q irrespective of $\theta_\mathbf{q}$ (Appendix B).

In addition to the CG mode, we obtain the other solution which has higher energy than the CG mode.[14] (In the following, it is referred as the upper mode.) At the present stage, the character of this mode is unclear except that, as shown in Fig. 2, the CG mode disappears with the upper mode at a low temperature. Since the upper mode does not appear as a peak in the spectrum of $S(\mathbf{q},\omega)$, we do not investigate it in this paper.

B. Velocity

Figure 2 shows the velocities of the CG mode v_{CG} and the phason v_ϕ. The difference between the two is small near T_c^0, because the Coulomb interaction is screened out by the quasiparticles. The anisotropy of v_{CG} becomes remarkable with decreasing temperature. Since $\theta_\mathbf{q}$ dependence of v_ϕ is weak compared with that of v_{CG}, we find that the effect of the charge-density fluctuation which is described by the last term in Eq. (2.11) ($\equiv V_{2332}$) is the dominant origin of this anisotropy.

The temperature region where the CG mode exists is very wide compared with that in the isotropic *s*-wave case as shown in Fig. 2(a). (For the isotropic *s*-wave state, we put $\gamma_\mathbf{p}=1$.) This is because the quasiparticles around the nodes can screen the Coulomb interaction down to lower temperatures in the *d*-wave state. We also find that, while v_{CG} increases with decreasing temperature in the isotropic *s*-wave state, it saturates at a value ($\equiv v_S$) depending on $\theta_\mathbf{q}$ in the *d*-wave one. The increase of v_{CG} in the former can be understood as that the phase of the order parameter becomes

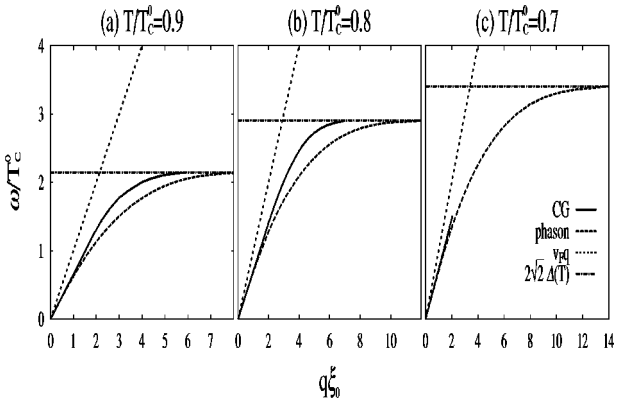

FIG. 1. Dispersion of the CG mode at $\theta_\mathbf{q}=0$.

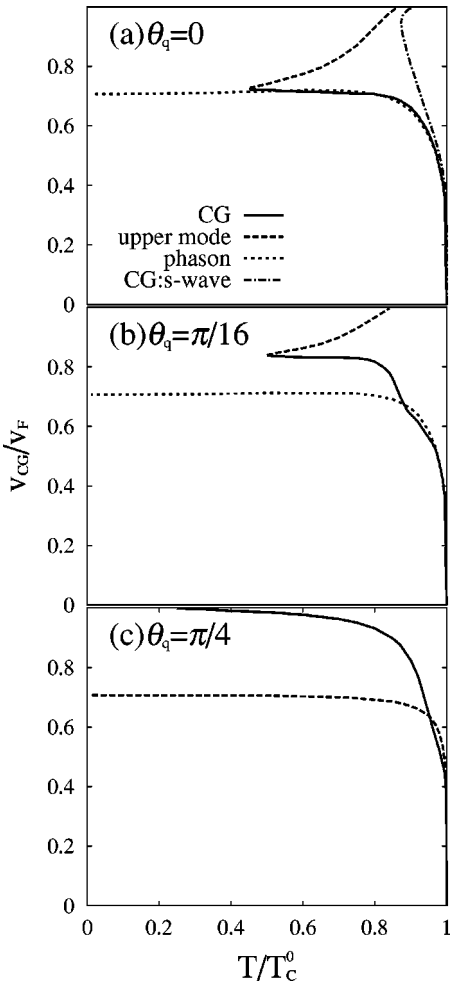

FIG. 2. Temperature dependence of the velocity of the collective phase oscillations. We have obtained the velocity as $v=\omega/q$ at $q\xi_0=0.2$. In the *s*-wave case, the CG mode and the upper mode are shown with the same dashed-dotted line.

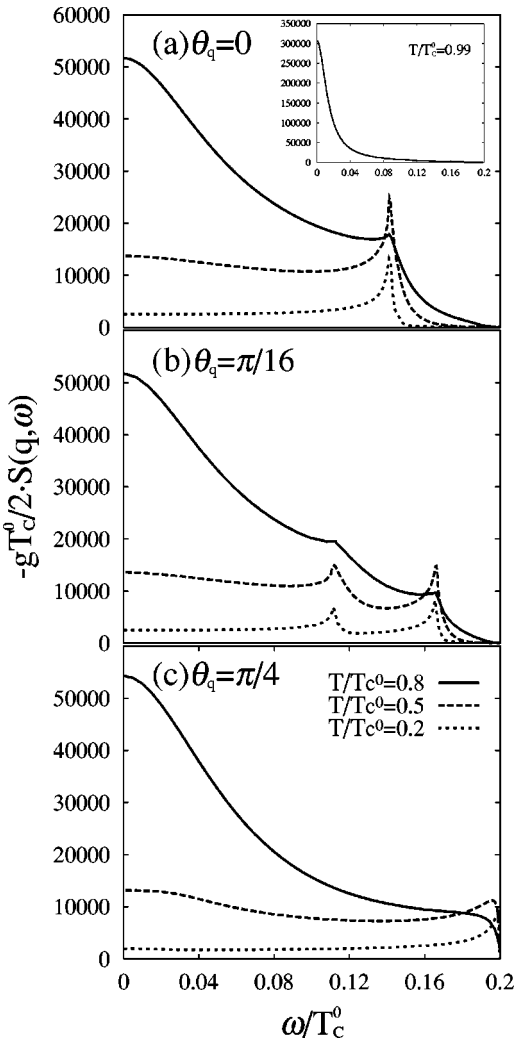

FIG. 3. Temperature dependence of $S(\mathbf{q},\omega)$ at $q\xi_0=0.2$ in charged *d*-wave superconductivity. Since $S(\mathbf{q},\omega)$ at $T=0.99T_c^0$ is almost $\theta_\mathbf{q}$ independent, only the spectrum at $\theta_\mathbf{q}=0$ is shown in the inset in (a).

''hard'' owing to the recovery of the long-range Coulomb interaction at low temperatures. On the other hand, v_S is well described by $v_S=v_F\cos\theta_1$, where $\theta_1\equiv\theta_\mathbf{q}-\pi/4$ is the angle of $\mathbf{q}$ measured from the nodal direction at $\theta=\pi/4$. Indeed, this equation gives

$$v_S=v_F\times\begin{cases}0.707 & (0.715 \text{ at } T=0.6T_c^0) & :\theta_\mathbf{q}=0,\\ 0.831 & (0.833 \text{ at } T=0.6T_c^0) & :\theta_\mathbf{q}=\pi/16,\\ 1 & (0.99 \text{ at } T=0.4T_c^0) & :\theta_\mathbf{q}=\pi/4,\end{cases} \tag{3.1}$$

where the numbers in the parentheses is v_{CG} in Fig. 2. Thus we find that the saturation of v_{CG} is deeply related to the nodes of the order parameter. We investigate this effect in detail in Sec. III.D.

C. Structure function of pair field susceptibility: $S(\mathbf{q},\omega)$

Figure 3 shows the temperature dependence of $S(\mathbf{q},\omega)$. At $T=0.99T_c^0$, the anisotropy of $S(\mathbf{q},\omega)$ is weak, because the thermal excitation of the quasiparticles is not restricted around the nodes but occurs in all directions in momentum space. Apart from slight difference, the spectrum is given by the inset in Fig. 3(a) irrespective of $\theta_\mathbf{q}$. We find that there is no peak structure except for the central peak at $\omega=0$.

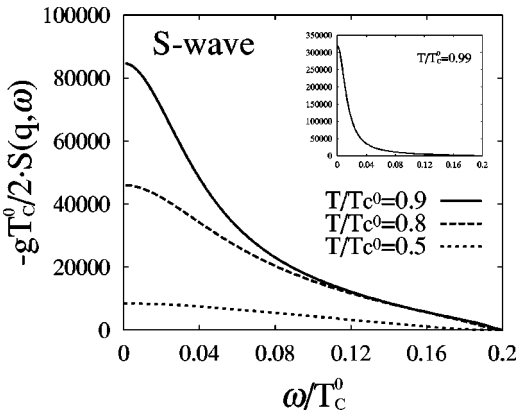

FIG. 4. Temperature dependence of $S(\mathbf{q},\omega)$ at $q\xi_0=0.2$ in two-dimensional charged *s*-wave superconductivity with $\gamma_\mathbf{p}=0$.

A peak structure begins to appear at a finite energy depending on $\theta_\mathbf{q}$ for $T\lesssim 0.8T_c^0$: The peak splits into two for $\theta_\mathbf{q}\neq 0$ as shown in Fig. 3(b). At $\theta_\mathbf{q}=\pi/4$, the higher peak is located near $\omega=0.2T_c^0$, while the lower one disappears.

We compare the peak energy at $T=0.5T_c^0$ with $\omega=v_{CG}q$ in which v_{CG} is given in Fig. 2:

$$\frac{\omega}{T_c^0}=\begin{cases}0.144 & (0.141) & :\theta_\mathbf{q}=0,\\ 0.168 & (0.112,\ 0.166) & :\theta_\mathbf{q}=\pi/16,\\ 0.197 & (0.196) & :\theta_\mathbf{q}=\pi/4,\end{cases} \tag{3.2}$$

where the numbers in the parentheses are the peak energies in Fig. 3. Thus except for the lower peak in Fig. 3(b), we find that the peaks correspond to the CG mode. We mention that this result is qualitatively different from that in the clean isotropic *s*-wave case in which, as shown in Fig. 4, the CG mode does not appear in the spectrum of $S(\mathbf{q},\omega)$.[14]

There is no pole which corresponds to the lower peak in Fig. 3(b). We note that it is not the ''upper mode.'' Instead, we find that the lower peak energy is well fitted with $\omega=v_S'q$, where $v_S'=v_F\cos\theta_2$. [$\theta_2\equiv\theta_\mathbf{q}-(-\pi/4)$: angle of $\mathbf{q}$ measured from the nodal direction at $\theta=-\pi/4$]: It gives $\omega=0.111T_c^0$ at $\theta_\mathbf{q}=\pi/16$. This agreement indicates that the node of the order parameter is a key also in understanding the lower peak. Furthermore, since the splitting of the peak is not observed in the neutral system (Fig. 5), V_{2332} is crucial also for the lower peak in Fig. 3(b).

D. Nodal effect on the CG mode

Now we investigate how the nodes of the order parameter affect the CG mode and $S(\mathbf{q},\omega)$. Focusing on $\Delta_\mathbf{p}=0$ at the nodes, we regard the nodes as two *one-dimensional normal-state electronic bands* toward $\theta=\pm\pi/4$, as schematically shown in Fig. 6.

These ''normal bands'' do not affect Π_{22}^0 and Π_{23}^0, because the basis function, $\gamma_\mathbf{p}=\sqrt{2}\cos(2\theta_\mathbf{p})$ in Eqs. (2.7) and (2.9) equals 0 at the nodes. On the other hand, they affect

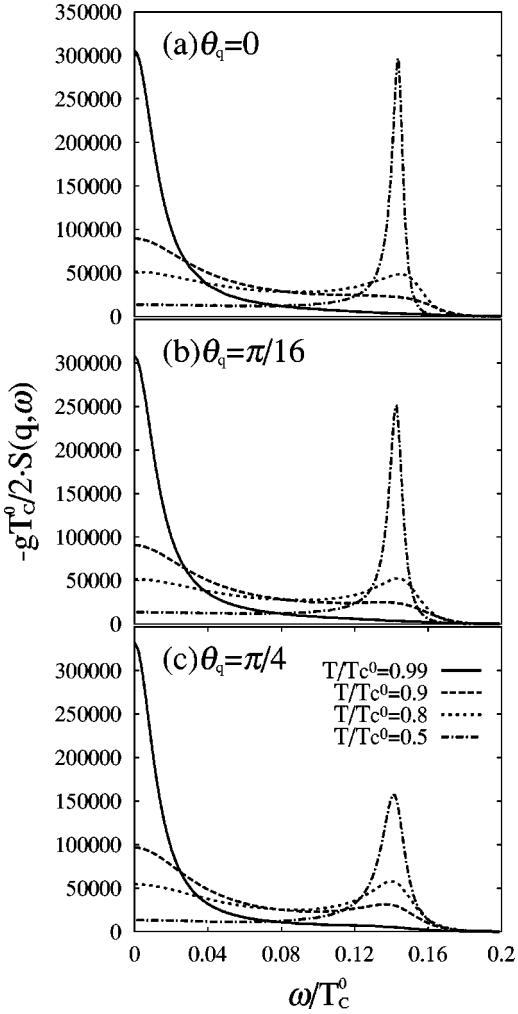

FIG. 5. Temperature dependence of $S(\mathbf{q},\omega)$ at $q\xi_0=0.2$ in neutral *d*-wave superconductivity.

Π_{33}^0, because $\gamma_{\mathbf{p}}$ is absent in Eq. (2.8). To see the effect of the normal bands, we extract only their contributions from $\Pi_{33}^0(\mathbf{q},\omega)$:

$$\Pi_{33}^{(1)}(\mathbf{q},\omega)\equiv -2N_1(0)\sum_{i=1,2}\frac{\eta_i^2}{\eta_i^2-\omega_+^2}, \tag{3.3}$$

where $\eta_i=v_F q_i$ with $q_i=q\cos\theta_i$; $N_1(0)$ is DOS of one of the one-dimensional bands at the Fermi level. Clearly, Eq. (3.3) diverges negatively in the limit $\omega\to\eta_i-\delta$. In this limit, the screened Coulomb interaction $V/(1-V\Pi_{33}^{(1)})$ is completely suppressed. Although the angular integration in Eq. (2.8) weakens the singularity, it still remains in Π_{33}^0 as shown in Fig. 7.

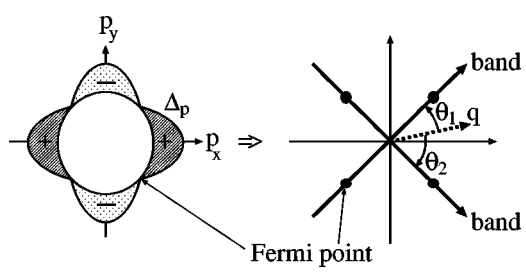

FIG. 6. Schematic picture of two one-dimensional normal electron bands in *d*-wave superconductivity.

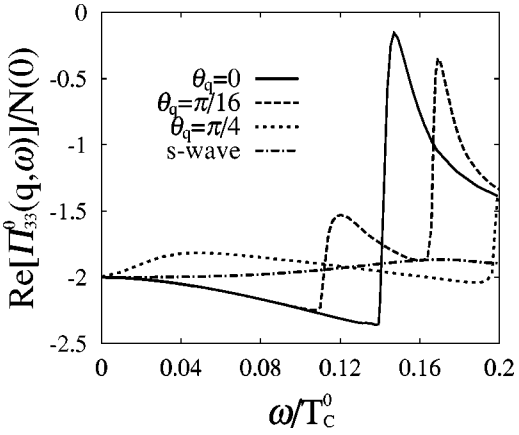

FIG. 7. Real part of $\Pi_{33}^0(\mathbf{q},\omega)$ in charged *d*-wave superconductivity. We put $T=0.5T_c^0$ and $q\xi_0=0.2$.

Figure 8 shows the spectrum of the real part of V_{2332}. In

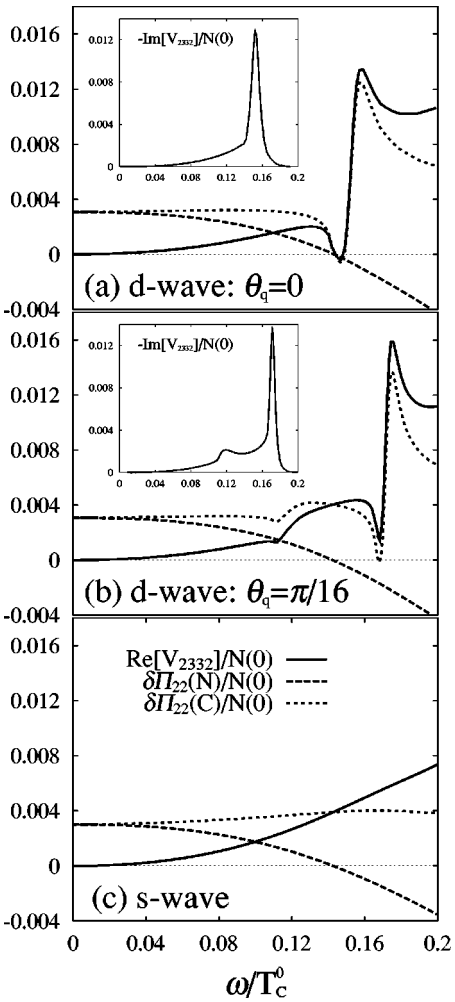

FIG. 8. Real part of $V_{2332}=\Pi_{23}^0[V/(1-V\Pi_{33}^0)]\Pi_{32}^0$ at $T=0.5T_c^0$ and $q\xi_0=0.2$. We also show $\delta\Pi_{22}(N)\equiv\mathrm{Re}[\Pi_{22}^0(\mathbf{q},\omega)-\Pi_{22}^0(0,0)]$ and $\delta\Pi_{22}(C)\equiv\mathrm{Re}[\overline{\Pi}_{22}^0(\mathbf{q},\omega)-\Pi_{22}^0(0,0)]=\delta\Pi_{22}^N+\mathrm{Re}[V_{2332}]$. The zeros of the former and the latter give the phason and the CG mode, respectively.

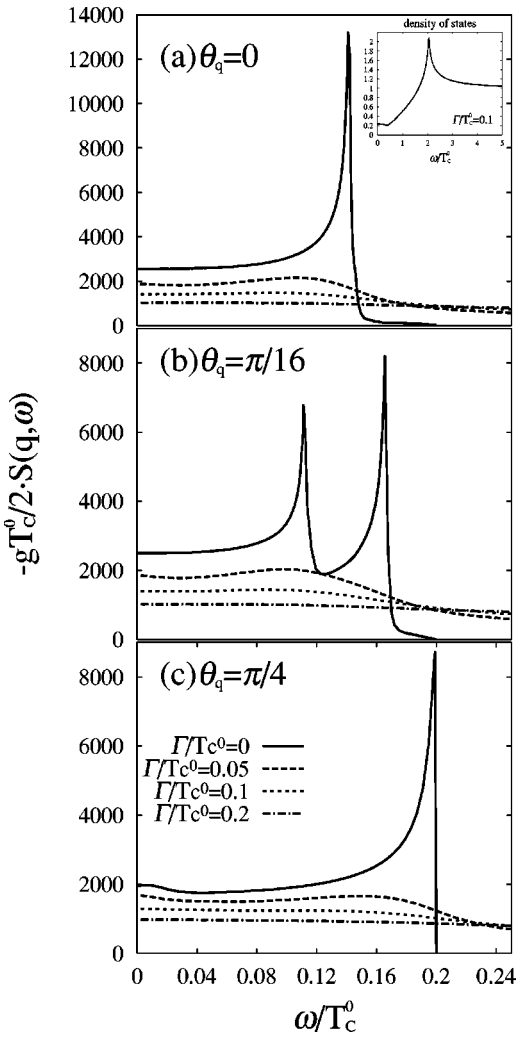

FIG. 9. Γ dependence of $S(\mathbf{q},\omega)$ in the unitarity limit. We put $T=0.2T_c$ and $q\xi_0=0.2$. The inset shows the superconducting DOS normalized by $N(0)$ for $\Gamma=0.1T_c^0$.

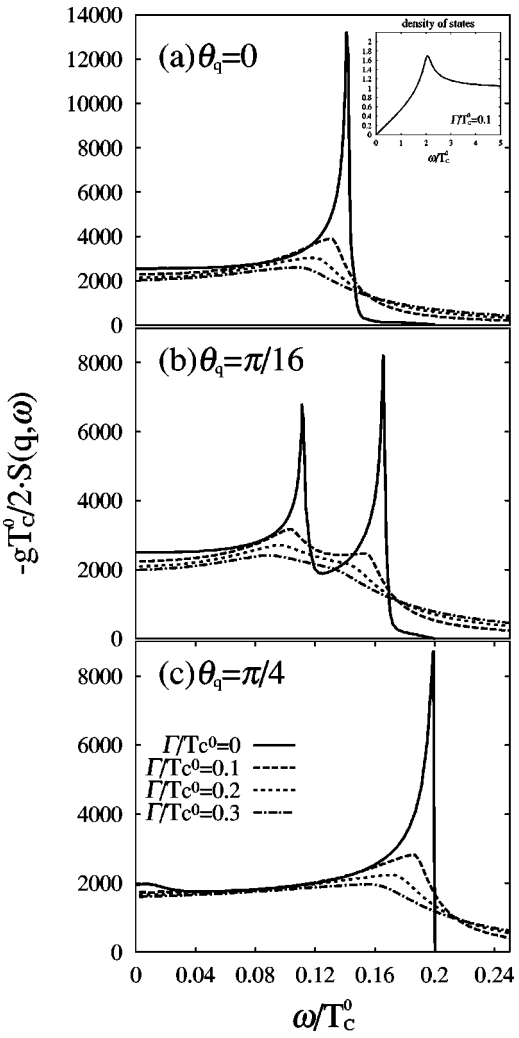

FIG. 10. Γ dependence of $S(\mathbf{q},\omega)$ in the case of the Born scattering. We put $T=0.2T_c$ and $q\xi_0=0.2$. The inset shows the superconducting DOS normalized by $N(0)$ for $\Gamma=0.1T_c^0$.

Figs. 8(a) and (b), we find that, as in the above simple discussion, the Coulomb interaction is suppressed around $\omega=\eta_i$: At $\theta_{\mathbf{q}}=0$, the effect of the two bands appears around $\omega=v_F q\cos(\pi/4)=0.141T_c^0$, while it appears $\omega=v_F q\cos(3\pi/16)=0.166T_c^0$ and $v_F q\cos(5\pi/16)=0.111T_c^0$ for $\theta_{\mathbf{q}}=\pi/16$. Then the CG mode is obtained even at $T=0.5T_c^0$ [$\delta\Pi_{22}(C)=0$ in Figs. 8(a) and 8(b)]. On the other hand, since this screening effect is absent in the isotropic *s*-wave state, $\delta\Pi_{22}(C)$ does not cross zero in Fig. 8(c).

The imaginary part of V_{2332} increases rapidly for $\omega\gtrsim\eta_i$ as a result of the singularity in Π_{33}^0, as shown in the insets in Figs. 8(a) and (b). Thus the imaginary part of the denominator of Eq. (2.11) also increases rapidly for $\omega\gtrsim\eta_i$. In addition, $\mathrm{Re}[\overline{\Pi}_{22}(\mathbf{q},\omega)-\Pi_{22}^0(0,0)]$ equals zero at the pole, and it is small also around $\omega=0.111T_c^0$ at $\theta_{\mathbf{q}}=\pi/16$. Thus $S(\mathbf{q},\omega)$ has a peak at $\omega\simeq\eta_i$ and decreases drastically for $\omega\gtrsim\eta_i$.

The saturation of v_{CG} in Fig. 2 is also attributed to the one-dimensional bands. Let us rewrite the equation of the CG mode as $\mathrm{Re}[\Pi_{22}^0(\mathbf{q},\omega)-\Pi_{22}^0(0,0)]+\mathrm{Re}[V_{2332}]=0$. Since $\mathrm{Re}[\Pi_{22}^0(\mathbf{q},\omega)-\Pi_{22}^0(0,0)]=0$ gives the phason in the neutral system, the ω dependence of $\mathrm{Re}[\Pi_{22}^0(\mathbf{q},\omega)-\Pi_{22}^0(0,0)]$ around $\omega=v_\phi q$ is almost T independent at low temperatures where $v_\phi\simeq v_F/\sqrt{2}$. Furthermore, $\mathrm{Re}[V_{2332}]$ is always suppressed around the same energy $\omega=\eta_i$. Therefore the energy of the CG mode is always located around $\omega=\eta_i$ at low temperatures.

Before ending this section, we briefly note that the same nodal effect occurs also in the extended *s*-wave state characterized by $\gamma_{\mathbf{p}}=\sqrt{2}|\cos(2\theta_{\mathbf{p}})|$ because the basis function appears as $\gamma_{\mathbf{p}}^2$ and $\gamma_{\mathbf{p}}\Delta_{\mathbf{p}}$ in Π_{ij}^0.

IV. COLLECTIVE PHASE OSCILLATION IN DIRTY SYSTEM

The peak in $S(\mathbf{q},\omega)$ is smeared by the impurity scatterings as shown in Fig. 9 (Born scattering) and Fig. 10 (unitaritylimit). When we again assume the two one-dimensional bands in Fig. 6, we obtain

$$\Pi_{33}^{(1)}(\mathbf{q},\omega)=-4N_1(0)\frac{(\eta_1^2-\overline{\omega^2})\eta_2^2+(\eta_2^2-\overline{\omega^2})\eta_1^2}{(\eta_1^2-\overline{\omega^2})(\eta_2^2-\omega_+\overline{\omega})+(\eta_2^2-\overline{\omega^2})(\eta_1^2-\omega_+\overline{\omega})}, \tag{4.1}$$

where $\overline{\omega}=\omega+i\Gamma$. We find that the singularity at $\omega=\eta_i$ is eliminated by Γ. As a result, the peak structure is suppressed by the impurity scatterings.

In the unitarity limit, the zero-energy bound states are induced around impurities,[29] so that the superconducting DOS becomes finite around $\omega=0$ (inset in Fig. 9). The induced quasiparticles around $\omega=0$ then cause the damping, which smears the peak structure in $S(\mathbf{q},\omega)$. On the other hand, the Born scattering does not cause the zero-energy bound state; the effect mainly appears around the region near the energy gap, $\omega=\sqrt{2}\Delta$ as far as Γ is small (see the inset in Fig. 10). Thus the smearing effect by the Born scattering on the CG mode being located in the low-energy region is weaker than that in the case of the unitarity limit.

When the temperature increases, the quasiparticles induced by the Born scattering around the energy gap begin to excite. Thus, even in the case of the Born scattering, the peak structure is smeared out by weaker Γ at higher temperatures. As an example, we show the Γ dependence of $S(\mathbf{q},\omega)$ at $T=0.5T_c$ in Fig. 11.

Figure 12 shows the Γ dependence of $S(\mathbf{q},\omega)$ just below T_c where, in the case of isotropic *s*-wave superconductivity, the CG mode appears in $S(\mathbf{q},\omega)$ in the dirty system (inset in Fig. 12).[5,12,14] In the *d*-wave superconductivity, only the central peak is observed at $\omega=0$. This is because the singularity in Π_{33}^0 is eliminated by Γ, and is because the depairing effect by the impurity scattering increases the quasiparticles which contribute to the damping of the CG mode.[30]

Although our theory is based on the *t*-matrix approximation, the singularity in Π_{33}^0 should be suppressed even if we treat the impurity scattering more correctly. Thus, at least qualitatively, we expect that the present tendency is not altered by more improved theories.

V. $S(\mathbf{q},\omega)$ IN *C* DIRECTION: JOSEPHSON PLASMA

A. Extension to quasi-two-dimensional system

In this section, we take into account a weak three dimensionality, and investigate $S(\mathbf{q},\omega)$ in the case when $\mathbf{q}$ is parallel to the *c* axis. It is known that the plasma energy can be very low in the *c* direction of quasi-two-dimensional systems.[31–35] This low-frequency plasma, the so-called Josephson plasma, is observed in high-T_c cuprates:[36–43] The observed plasma energy is lower than the energy gap.[43] Furthermore, the temperature dependence of the plasma energy in high-T_c cuprates indicates the presence of a scattering mechanism in the *c*-axis charge dynamics.[21] In the following, we investigate how the Josephson plasma affects $S(\mathbf{q},\omega)$ in dirty quasi-two-dimensional *d*-wave superconductivity.

In order to take into account weak three dimensionality of the system, we assume a simple effective-mass model:[21,33,34] We add a dispersion in the *c* direction $p_z/(2m_z)(m_z\gg m)$ to the kinetic energy $\xi_{\mathbf{p}}$. Then we cut the Fermi surface at the Brillouin-zone boundary at $p_z=\pm\pi$ to obtain an open quasi-two-dimensional Fermi surface.

In the dirty system, the formulation for the two-dimensional system is still valid except that $W_{\pm}^{ij}$ in Eq. (2.20) is replaced by

$$\begin{pmatrix} \overline{W}_{\pm}^{22} & \overline{W}_{\pm}^{23} \\ \overline{W}_{\pm}^{32} & \overline{W}_{\pm}^{33} \end{pmatrix} = \frac{\pi i}{2\overline{v}q}\ln\left[\frac{\sqrt{Z(\omega'_+ +\omega)^2-\Delta_{\mathbf{p}}^2}\pm\sqrt{Z(\omega'_\pm)^2-\Delta_{\mathbf{p}}^2}-\overline{v}q}{\sqrt{Z(\omega'_+ +\omega)^2-\Delta_{\mathbf{p}}^2}\pm\sqrt{Z(\omega'_\pm)^2-\Delta_{\mathbf{p}}^2}+\overline{v}q}\right]$$
$$\times\left[\tau_3\pm\frac{Z(\omega'_+ +\omega)Z(\omega'_\pm)-\Delta_{\mathbf{p}}^2+[Z(\omega'_+ +\omega)-Z(\omega'_\pm)]\Delta_{\mathbf{p}}\tau_2}{\sqrt{Z(\omega'_+ +\omega)^2-\Delta_{\mathbf{p}}^2}\sqrt{Z(\omega'_\pm)^2-\Delta_{\mathbf{p}}^2}}\right], \tag{5.1}$$

where $\overline{v}=\pi/m_z$, and we have put $\mathbf{q}=(0,0,q)$. We express $\overline{V}$ with use of the plasma energy along the *c* axis in the clean system $\omega_p^z=\sqrt{4\pi\delta n e^2/m_z}$ as $\overline{V}=(3/2)\cdot(\omega_p^z/T_c^0)^2/(q\xi_z)^2$,[21,33,34] where $\delta n=(\pi/3)(m/m_z)$ is the conductive carrier density in the *c* direction and $\xi_z\equiv\overline{v}/T_c^0$. Since δn can be much smaller than the total carrier density *n* in the quasi-two-dimensional system, ω_p^z can be much lower than the plasma energy in the in-plane direction. In the following, we put $\omega_p^z=0.05T_c^0$ in order to describe the low-frequency plasma.

B. $S(\mathbf{q},\omega)$ in *c* direction

Figure 13 shows the temperature dependence of $S(\mathbf{q},\omega)$ when $\mathbf{q}$ is parallel to the *c* axis. As in the case of the in-plane direction, we find a peak structure at low temperatures. However, this mode does not have a linear dispersion, but has the finite energy $\omega\simeq\omega_p^z$ at $q=0$ (Fig. 14). Thus this is the Josephson plasma oscillation.

Although there are four *line* nodes running along the *c* axis, there is no remarkable nodal effect in Figs. 13 and 14; results similar to these figures are obtained also in the dirty quasi-two-dimensional isotropic *s*-wave superconductivity.[33]

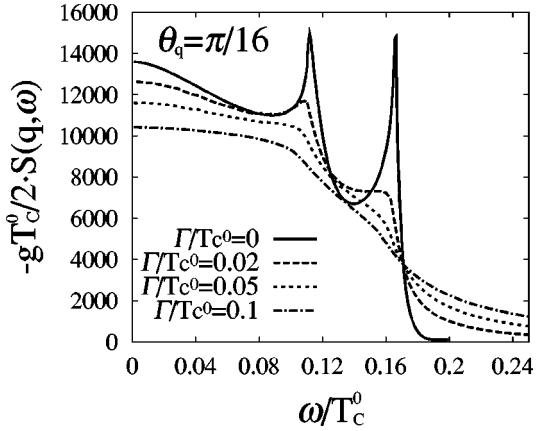

FIG. 11. Γ dependence of $S(\mathbf{q},\omega)$ at $T=0.5T_c$ and $\theta_{\mathbf{q}}=\pi/16$ in the case of the Born scattering.

When we regard them as two *two*-dimensional normal electron bands, and extract their contribution from Π_{33}^{Γ}, we obtain

$$\Pi_{33}^{(2)}=-4N_2(0)\left[1+\frac{\omega_+}{2\overline{vq}}\frac{\ln\left[\frac{\omega+i\Gamma-\overline{vq}}{\omega+i\Gamma+\overline{vq}}\right]}{1+\frac{i\Gamma}{2\overline{vq}}\ln\left[\frac{\omega+i\Gamma-\overline{vq}}{\omega+i\Gamma+\overline{vq}}\right]}\right], \tag{5.2}$$

where $N_2(0)$ is DOS of one of the two-dimensional bands at the Fermi level. At $\Gamma=0$, Eq. (5.2) diverges *positively* and logarithmically for $\omega\to\overline{vq}-\delta$. Thus the strong screening effect which is obtained in Eq. (3.3) is absent in the present

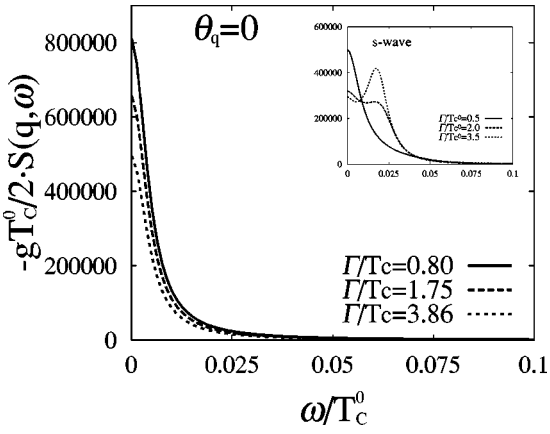

FIG. 12. Γ dependence of $S(\mathbf{q},\omega)$ at $T=0.999T_c$ and $q\xi_0=0.2$ in charged *d*-wave superconductivity. Since results for the Born scattering and the unitarity limit are almost the same, only the former case is shown. We note that the values of Γ shown in this figure are normalized by, not T_c^0, but T_c which is the transition temperature in the presence of the impurity scatterings. When we normalize Γ by T_c^0, 0.80, 1.75, 3.86 become 0.6, 1.0, and 1.4, respectively. The inset shows $S(\mathbf{q},\omega)$ at $T=0.999T_c^0$ and $q\xi_0=0.2$ in the case of two-dimensional charged *s*-wave superconductivity with $\gamma_{\mathbf{p}}=1$. A peak at a finite energy is the CG mode. Formulation for the *s*-wave state is explained in Appendix C.

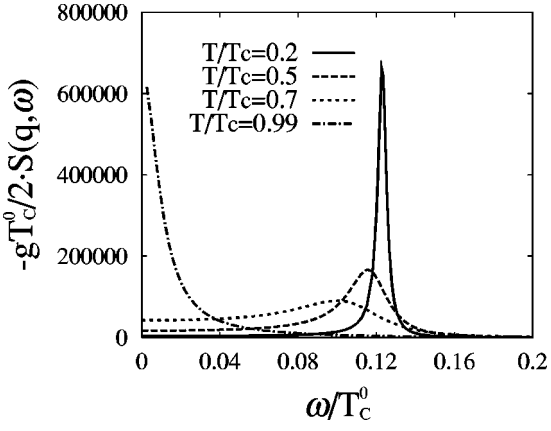

FIG. 13. Temperature dependence of $S(\mathbf{q},\omega)$ for $\mathbf{q}=(0,0,0.2\xi_z^{-1})$. The figure shows the case of the Born scattering. We put $\Gamma=0.1T_c^0$.

case. This logarithmic divergence is easily suppressed by Γ and the angular integration which we have neglected in Eq. (5.2).

Figure 15 shows the Γ-dependence of $S(\mathbf{q},\omega)$. We find that the plasma peak is not smeared by the impurity scatterings in contrast to the peak of the CG mode in the *d*-wave state. This is because, in the dirty system ($\omega_p^z\ll\Gamma$), the plasma is the oscillation of only the superfluid component which is not accompanied by dissipation.[33,34] On the other hand, since the depairing effect decreases the superfluid carrier density, the peak energy in Fig. 15, or the plasma energy, is lowered by Γ.

VI. SUMMARY AND DISCUSSION

In this paper, we showed that the character of the CG mode is much different in-between the *d*-wave and isotropic *s*-wave superconductors. In the former state, the CG mode can be observed in $S(\mathbf{q},\omega)$ at low temperatures in the clean system. This is due to the presence of four ''Fermi points'' at the nodes of the *d*-wave order parameter. They work as if there are two one-dimensional normal electric bands, which cause a singularity in the charge-density fluctuation to lead to a strong screening effect. This effect is suppressed in the

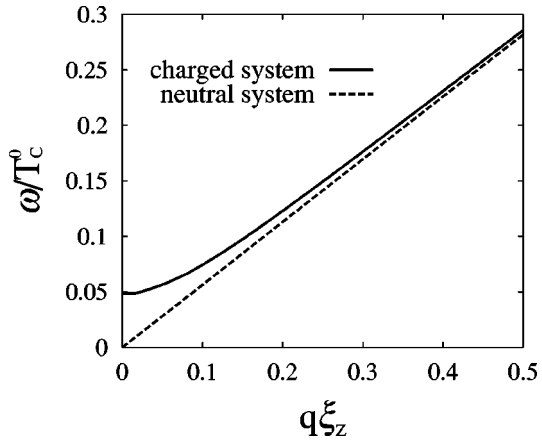

FIG. 14. Dispersion of the collective mode (plasma oscillation) in the *c* direction which is obtained from Eq. (2.20). We put $T=0.2T_c$, $\Gamma=0.1T_c^0$, and the Born scattering is assumed.

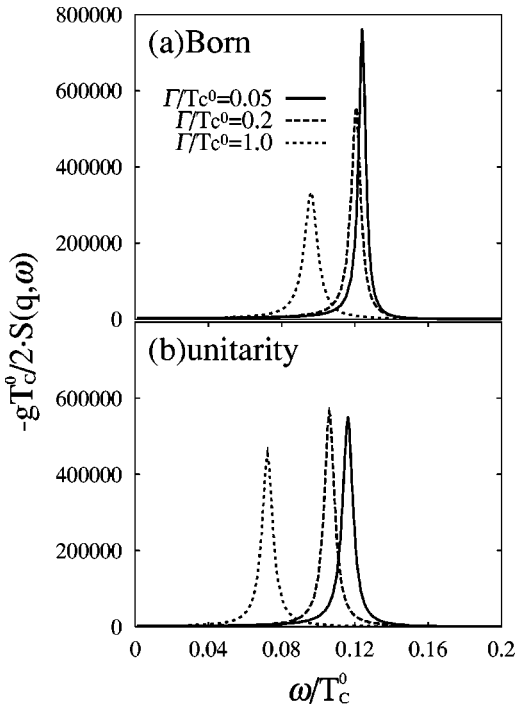

FIG. 15. Γ dependence of $S(\mathbf{q},\omega)$ for $\mathbf{q}=(0,0,0.2\xi_z^{-1})$ at $T=0.2T_c$.

dirty system. On the other hand, the CG mode is observed just below T_c in the dirty system in the isotropic *s*-wave state. We also showed that, when $\mathbf{q}$ is toward the *c* direction, instead of the CG mode, the plasma oscillation can be observed in $S(\mathbf{q},\omega)$.

When we apply the present results to high-T_c cuprates, we should take into account the anisotropy of the electronic state: If DOS in the normal state is negligibly small around the nodes compared with DOS around $(\pm\pi,0)$ and $(0,\pm\pi)$ in real systems, the nodal effect discussed in this paper is suppressed. In other cases, it should remain. In the latter case, since the high-T_c cuprate superconductors are known to be near the clean limit in the in-plane direction (mean free path $l\sim 100[A]\gg\xi\sim 10[A]$), and since, far below T_c, the inelastic scattering by the antiferromagnetic spin fluctuations is suppressed by the presence of the excitation gap, the CG mode may be observed in the in-plane direction of high-T_c cuprates. In addition, since the detailed Fermi surface in the in-plane direction is not crucial for the Josephson plasma in the *c* direction, we can expect that the Josephson plasma which has been observed by the microwave experiments may be observed in high-T_c cuprates also by the tunneling experiment which was developed for the CG mode.

APPENDIX A: CALCULATION OF Π_{22}^{Γ} IN DIRTY SYSTEM

The polarization function Π_{ij}^{Γ} is given by

$$\Pi_{ij}^{\Gamma}(\mathbf{q},i\nu_n)=\frac{1}{\beta}\sum_{\mathbf{p},\omega_m}\mathrm{Tr}[\tau_i\gamma_{\mathbf{p}}^{i}\tilde{G}(p+q/2)\Gamma^{j}_{p+q/2,p-q/2}\tilde{G}\times(p-q/2)], \tag{A1}$$

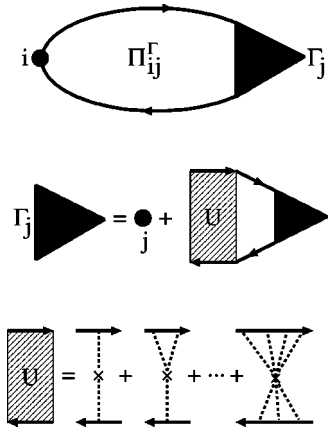

FIG. 16. Feynman diagram for Π_{ij}^{Γ} within the *t*-matrix approximation. The solid line represents the renormalized Green's function, $\tilde{G}$, which includes the self-energy part. The bare vertex $\tau_i\gamma_{\mathbf{p}}^{i}$ is expressed by the solid circle, while ''×'' represents an impurity. The four point vertex *U* describes the multiscattering by impurities (dashed line).

where $\Gamma^{j}_{p+q/2,p-q/2}$ is the vertex correction for $\tau_j\gamma_{\mathbf{p}}^{j}$; we have simply written $p+q/2=(\mathbf{p}+\mathbf{q}/2,\omega_m+\nu_n)$, $p-q/2=(\mathbf{p}-\mathbf{q}/2,\omega_m)$. In the following, we consider $\Pi_{ij}^{\Gamma}(\mathbf{q},i\nu_n)$ with $i,j=0,1,2,3$; for $i=0$ and/or $j=0$, $\tau_0=1$ and $\gamma_{\mathbf{p}}^{0}=1$ are used in Eq. (A1).

1. Vertex correction

The vertex correction $\Gamma^{j}_{p+q/2,p-q/2}$ within the *t*-matrix approximation is diagrammatically given by Fig. 16. Summing up the impurity scatterings in *U* in Fig. 16, we obtain

$$\Gamma^{j}_{p+q/2,p-q/2}=\tau_j\gamma_{\mathbf{p}}^{j}+n_i\sum_{\mathbf{k}}\tilde{u}(i\omega_m+i\nu_n)\tilde{G}\times(k+q/2)\Gamma^{j}_{k+q/2,k-q/2}\tilde{G}(k-q/2)\tilde{u}(i\omega_m), \tag{A2}$$

where $k+q/2=(\mathbf{k}+\mathbf{q}/2,\omega_m+\nu_n)$, and $k-q/2=(\mathbf{k}-\mathbf{q}/2,\omega_m)$. The function $\tilde{u}$ is given by

$$\tilde{u}(i\omega_m)=u\tau_3\frac{1}{1-u\sum_{\mathbf{p}}\tilde{G}(\mathbf{p},i\omega_m)\tau_3}=\frac{1}{\pi N(0)}\frac{C\tau_3-\Lambda(i\omega_m)}{C^2-\Lambda^2(i\omega_m)}. \tag{A3}$$

Since the last term in Eq. (A2) is independent of $\mathbf{p}$, we can write

$$\Gamma^{j}_{p+q/2,p-q/2}=\tau_j\gamma_{\mathbf{p}}^{j}+f_j(q,i\omega_m), \tag{A4}$$

where $q=(\mathbf{q},i\nu_n)$, and

$$f_j(q,i\omega_m)=n_i\sum_{\mathbf{k}}\tilde{u}(i\omega_m+i\nu_n)\tilde{G}(k+q/2)\tau_j\gamma_{\mathbf{k}}^j\tilde{G}\times(k-q/2)\tilde{u}(i\omega_m)+n_i\sum_{\mathbf{k}}\tilde{u}(i\omega_m+i\nu_n)\tilde{G}\times(k+q/2)\tau_j f_j(q,i\omega_m)\tilde{G}(k-q/2)\tilde{u}(i\omega_m). \tag{A5}$$

When we expand $f_j(q,i\omega_m)$ as $f_j(q,i\omega_m)=\Sigma_{l=0}^{3}F_{jl}(q,i\omega_m)\tau_j$, F_{jl} satisfies[10,14]

$$\sum_{l=0}^{3}F_{jl}(q,i\omega_m)\left[\delta_{jn}-n_iN(0)\sum_{r=0}^{3}S_{lr}E_{rn}\right]=n_iN(0)\sum_{r=0}^{3}\tilde{S}_{jr}E_{rn}, \tag{A6}$$

where

$$S_{lr}=\frac{1}{2N(0)}\sum_{\mathbf{k}}\mathrm{Tr}[\tilde{G}(k+q/2)\tau_l\tilde{G}(k-q/2)\tau_r],$$

$$\tilde{S}_{jr}=\frac{1}{2N(0)}\sum_{\mathbf{k}}\mathrm{Tr}[\tilde{G}(k+q/2)\tau_j\gamma_{\mathbf{k}}^j\tilde{G}(k-q/2)\tau_r],$$

$$E_{lr}(i\omega_m+i\nu_n,i\omega_m)=\frac{1}{2}\mathrm{Tr}[\tilde{u}(i\omega_m+i\nu_n)\tau_l\tilde{u}(i\omega_m)\tau_r]. \tag{A7}$$

In Eq. (A7), the trace is taken with respect to the Pauli matrices. Introducing 4×4 matrices, $F\equiv\{F_{ij}\}$, $S\equiv\{S_{ij}\}$, $\tilde{S}\equiv\{\tilde{S}_{ij}\}$, and $E\equiv\{E_{ij}\}$ $(i,j=0\sim3)$, F is obtained as $F=n_iN(0)\tilde{S}E[1-n_iN(0)SE]^{-1}$.

2. Π_{ij}^{Γ}

Substituting Eq. (A4) into Eq. (A1), we obtain

$$\Pi_{ij}^{\Gamma}(\mathbf{q},i\nu_n)=\frac{1}{\beta}\sum_{\mathbf{p},\omega_m}\mathrm{Tr}[\tau_i\gamma_{\mathbf{p}}^j\tilde{G}(p+q/2)\tau_j\gamma_{\mathbf{p}}^j\tilde{G}(p-q/2)]+\frac{1}{\beta}\sum_{\mathbf{p},\omega_m,l}F_{jl}(\mathbf{q},i\omega_m,i\nu_n)\times\mathrm{Tr}[\tau_i\gamma_{\mathbf{p}}^j\tilde{G}(p+q/2)\tau_l\tilde{G}(p-q/2)]. \tag{A8}$$

When we rewrite the last term in Eq. (A8) with use of

$$\overline{S_{lr}^{i}}=\frac{1}{2N(0)}\sum_{\mathbf{p}}\gamma_{\mathbf{p}}^i\mathrm{Tr}[\tilde{G}(p+q/2)\tau_l\tilde{G}(p-q/2)\tau_r], \tag{A9}$$

only the term with $i=r$ remains because of $\mathrm{Tr}[\tau_i\tau_r]=2\delta_{ir}$. In the following, we simply write $\overline{S_{li}^{i}}$ as $\overline{S_{li}}$. Equation (A8) then becomes

$$\Pi^{\Gamma}=\frac{2N(0)}{\beta}\sum_{\omega_m}\{\hat{A}+n_iN(0)\overline{A}[1-n_iN(0)\overline{E}\overline{A}]^{-1}\overline{E}\tilde{A}\}, \tag{A10}$$

where $\Pi^{\Gamma}\equiv\{\Pi_{ij}^{\Gamma}\}$, $A={}^tS$, $\tilde{A}={}^t\tilde{S}$, $\overline{A}=\{\overline{S_{ji}}\}$, and the matrix element of $\hat{A}$ is given by

$$\hat{A}_{ij}=\frac{1}{2N(0)}\sum_{\mathbf{p}}\mathrm{Tr}[\tau_i\gamma_{\mathbf{p}}^i\tilde{G}(p+q/2)\tau_j\gamma_{\mathbf{p}}^j\tilde{G}(p-q/2)]. \tag{A11}$$

3. Expressions for Born scattering and unitarity limit

a. $\overline{E}$

In the cases of the Born scattering ($C\gg1$) and the unitarity limit ($C=0$), Eq. (A3) is respectively reduced to

$$\tilde{u}(i\omega_m)=\begin{cases}\dfrac{1}{\pi N(0)C}\tau_3=u\tau_3 & \text{(Born)},\\ \dfrac{1}{\pi N(0)\Lambda(i\omega_m)} & \text{(unitarity)}.\end{cases} \tag{A12}$$

Then $\overline{E}_{ij}$ is given by

$$\overline{E}_{ij}^{\mathrm{Born}}=u^2\begin{pmatrix}\tau_3 & 0\\ 0 & -\tau_3\end{pmatrix},$$

$$\overline{E}_{ij}^{\mathrm{unitarity}}=\frac{1}{\Lambda(i\omega_m+i\nu_n)\Lambda(i\omega_m)}\left(\frac{1}{\pi N(0)}\right)^2\begin{pmatrix}\mathbf{1} & 0\\ 0 & \mathbf{1}\end{pmatrix}. \tag{A13}$$

b. ξ integration

We transform the $\mathbf{p}$ summation in Π^{Γ} into the ξ and angular integrations, and execute the former integration. In this procedure, we mention that, in principle, we must execute the ω_m summation before the ξ integration, because the commutability of the two calculations is not guaranteed. Thus, when we exchange the two procedures in our calculation, we must carefully treat the commutability. In the present case, the uncommutability occurs in Π_{33}^{Γ}.[14] In order to avoid this uncommutability, we write Π_{33}^{Γ} as[14]

$$\Pi_{33}^{\Gamma}=[\Pi_{33}^{\Gamma}-\Pi_{33}^{\Gamma N}]_{\xi}+\Pi_{33}^{\Gamma N}, \tag{A14}$$

where $\Pi_{33}^{\Gamma N}$ represents Π_{33}^{Γ} in the normal state, which is given by Eq. (2.17).[14] Since $[\Pi_{33}^{\Gamma}-\Pi_{33}^{\Gamma N}]$ well converges, we can execute the ξ integration before the ω_m summation in it; the subscript ξ in Eq. (A14) represents this exchange.

When we execute the ξ integration, we find that A, $\tilde{A}$, $\overline{A}$, and $\hat{A}$ have the block-diagonalized form as

$$\begin{pmatrix}a_{00} & a_{01} & 0 & 0\\ a_{10} & a_{11} & 0 & 0\\ 0 & 0 & a_{22} & a_{23}\\ 0 & 0 & a_{32} & a_{33}\end{pmatrix}. \tag{A15}$$

Thus, as far as Eq. (A13) is considered, the upper and the lower blocks in Eq. (A15) do not mix with each other in calculating Eq. (A10). Since we need only the lower 2×2 block in Π^{Γ} [$\leftrightarrow$ Eq. (2.16)], we extract this part:

$$\begin{pmatrix} \Pi^{\Gamma}_{22} & \Pi^{\Gamma}_{23} \\ \Pi^{\Gamma}_{32} & \Pi^{\Gamma}_{33} \end{pmatrix}_{\xi} = \frac{2N(0)}{\beta}\sum_{\omega_m} \times\{\hat{A}-\overline{A}[1+\alpha(i\omega_m,i\nu_n)A]^{-1}\alpha \times(i\omega_m,i\nu_n)\tilde{A}\}, \tag{A16}$$

where $\alpha(i\omega_m,i\nu_n)$ is given by Eq. (2.22). In Eq. (A16), A, $\overline{A}$, $\tilde{A}$, and $\hat{A}$ are now 2×2 matrices with the matrix elements being arranged as Eq. (2.19); their expressions are given by Eq. (2.20) in which the subscript ''$\pm$'' being eliminated, $\omega \rightarrow i\nu_n$, and $\omega' \rightarrow i\omega_m$.

c. ω_m summation and analytic continuation

We calculate the ω_m summation in the same way as that in the case of the *s*-wave superconductivity:[14] We transform the summation into the complex integration in the ordinary manner. After avoiding branch cuts on the complex plane, we put $i\nu_n \rightarrow \omega + i\delta$. Then, except for $\Pi^{\Gamma}_{33\xi}$, Eq. (A16) is reduced to the second term in Eq. (2.16). In $\Pi^{\Gamma}_{33\xi}$, in addition to the second term in Eq. (2.16), there is an extra term coming from a complex integration along the infinitely large contour;[14] however, it is canceled by $\Pi^{\Gamma N}_{33\xi}$ in Eq. (A14). Thus $[\Pi^{\Gamma}_{33}-\Pi^{\Gamma N}_{33}]_{\xi}$ gives the second term in Eq. (2.16). Taking account the last term in Eq. (A14), we obtain Eq. (2.16).

APPENDIX B: PHASON AT $T=0$ IN TWO-DIMENSIONAL SYSTEM

The equation of the phason is $\Pi^{0}_{22}(\mathbf{q},\omega)-\Pi^{0}_{22}(0,0)=0$. At $T=0$, the first line in the right-hand side of Eq. (2.7) is absent. We put $\omega = v_{\phi}q$, and then expand the second line in Eq. (2.7) in terms of q up to the second order:

$$\Pi^{0}_{22}(\mathbf{q},\omega)-\Pi^{0}_{22}(0,0) \simeq -\frac{N(0)}{2\Delta^2}\left[v_{\phi}^2-\frac{1}{2}(v_{\mathrm{F}})^2\right]q^2. \tag{B1}$$

Thus we obtain $v_{\phi}=v_{\mathrm{F}}/\sqrt{2}$.

In the charged system, when we expand V_{2332} as in the above, we obtain $V_{2332}=N(0)/(2\Delta^2)\cdot(v_{\mathrm{CG}}q)^2$ at $T=0$. Then we obtain $v_{\mathrm{CG}}=\infty$, which means the absence of the CG mode at $T=0$.

APPENDIX C: Π_{22} IN DIRTY TWO-DIMENSIONAL *S*-WAVE SUPERCONDUCTIVITY

The derivation of Π_{22} for a dirty two-dimensional *s*-wave superconductivity is the same as that in our previous paper for a three-dimensional one:[14] We replace the second term in the right-hand side of Eq. (2.16) by $\Pi^{\Gamma}_{\mathrm{M}}$ which is given by Eq. (B.20) in Ref. 14. In Eq. (B.20), the average is now taken over the two-dimensional Fermi surface. Then we obtain

$$\begin{aligned}\Pi^{\Gamma}_{\mathrm{M}} = &-N(0)\int_{-\infty}^{\infty}d\omega'\tanh\frac{\beta\omega'}{2}\left[\tau_3+\frac{(\omega'_{+}+\omega)\omega'_{+}-\Delta^2+\Delta\omega\tau_2}{\sqrt{(\omega'_{+}+\omega)^2-\Delta^2}\sqrt{\omega'^{\,2}_{+}-\Delta^2}}\right] \\ &\times\frac{1}{\sqrt{[\sqrt{(\omega'_{+}+\omega)^2-\Delta^2}+\sqrt{\omega'^{\,2}_{+}-\Delta^2}+i\Gamma]^2-(v_{\mathrm{F}}q)^2}-i\Gamma} \\ &+N(0)\int_{-\infty}^{\infty}d\omega'\tanh\frac{\beta\omega'}{2}\left[\tau_3-\frac{(\omega'_{+}+\omega)\omega'_{-}-\Delta^2+\Delta\omega\tau_2}{\sqrt{(\omega'_{+}+\omega)^2-\Delta^2}\sqrt{\omega'^{\,2}_{-}-\Delta^2}}.\right] \\ &\times\frac{1}{\sqrt{[\sqrt{(\omega'_{+}+\omega)^2-\Delta^2}-\sqrt{\omega'^{\,2}_{-}-\Delta^2}+i\Gamma]^2-(v_{\mathrm{F}}q)^2}-i\Gamma}.\end{aligned} \tag{C1}$$

[1] P. W. Anderson, Phys. Rev. **110**, 827 (1958); **112**, 1900 (1958).
[2] R. V. Carlson and A. M. Goldman, Phys. Rev. Lett. **31**, 880 (1973); **34**, 11 (1975); J. Low Temp. Phys. **25**, 67 (1976).
[3] F. E. Aspen and A. M. Goldman, J. Low Temp. Phys. **43**, 559 (1981).
[4] P. W. Anderson, Phys. Rev. **130**, 439 (1963).
[5] A. Schmid and G. Schön, Phys. Rev. Lett. **34**, 941 (1975).
[6] S. N. Artemenko and A. F. Volkov, Zh. Éksp. Teor. Fiz. **69**, 1764 (1975) [Sov. Phys. JETP **42**, 896 (1975)].
[7] C. J. Pethick and H. Smith, Ann. Phys. (N.Y.) **119**, 133 (1979).
[8] A. M. Kadin, L. N. Smith, and W. J. Skocpol, J. Low Temp. Phys. **38**, 497 (1980).
[9] M. Dinter, J. Low Temp. Phys. **26**, 557 (1974); **32**, 529 (1978); Phys. Rev. B **18**, 3163 (1978).
[10] I. O. Kulik, Entin-Wohlman, and R. Orbach, J. Low Temp. Phys. **43**, 591 (1981).
[11] O. D. Cheishvili, J. Low Temp. Phys. **48**, 445 (1982).
[12] G. Schön, *Nonequilibrium Superconductivity*, edited by D. N. Langenberg and A. I. Larkin (Elsevier Science Publishers, Amsterdam, 1986), Chap. 13, and references therein.
[13] K. Y. M. Wong and S. Takada, Phys. Rev. B **37**, 5644 (1988).
[14] Y. Ohashi and S. Takada, J. Phys. Soc. Jpn. **66**, 2437 (1997).
[15] R. A. Ferrel, J. Low Temp. Phys. **1**, 423 (1969).
[16] D. J. Scalapino, Phys. Rev. Lett. **24**, 1052 (1970).
[17] H. Takayama, Prog. Theor. Phys. **46**, 1 (1971).

[18] S. R. Shenoy and P. A. Lee, Phys. Rev. B **10**, 2744 (1974).
[19] D. J. van Harlingen, Rev. Mod. Phys. **67**, 515 (1995).
[20] S. N. Artemenko and A. G. Kobelkov, Phys. Rev. B **55**, 9094 (1997).
[21] Y. Ohashi and S. Takada, J. Phys. Soc. Jpn. **67**, 551 (1998).
[22] The expression of $V(\mathbf{q})$ depends on a model. For example, $V(\mathbf{q})=2\pi e^2/q$ for a purely two-dimensional case, while

$$V(\mathbf{q})=\frac{2\pi de^2}{q_\parallel}\frac{\sinh(dq_\parallel)}{\cosh(dq_\parallel)-\cos(dq_z)}(q_\parallel=\sqrt{q_x^2+q_y^2})$$

for a layered system in the absence of the interlayer electron tunneling (d: interlayer spacing) [H. A. Fertig and S. D. Sarma, Phys. Rev. B **44**, 4480 (1991)]. However, the detailed expression is not crucial for the CG mode, because it appears when the Coulomb interaction is screened out by the quasiparticles. Although we do not show the $V(\mathbf{q})$ dependence of our results explicitly, they do not depend on the choice of $V(\mathbf{q})$.
[23] C. Bruder, Phys. Rev. B **41**, 4017 (1990).
[24] S. Schmitt-Rink, K. Miyake, and C. M. Varma, Phys. Rev. Lett. **57**, 2575 (1986).
[25] P. J. Hirschfeld, D. Vollhardt, and P. Wölfle, Solid State Commun. **59**, 111 (1986).
[26] P. J. Hirschfeld, P. Wölfle, and D. Einzel, Phys. Rev. B **37**, 83 (1988).
[27] P. J. Hirschfeld, W. O. Putikka, and D. J. Scalapino, Phys. Rev. B **50**, 10 250 (1994).
[28] P. J. Hirschfeld, S. M. Quinlan, and D. J. Scalapino, Phys. Rev. B **55**, 12 742 (1997).
[29] Y. Onishi, Y. Ohashi, Y. Shingaki, and K. Miyake, J. Phys. Soc. Jpn. **65**, 675 (1996).
[30] At the present stage, we cannot exclude the possibility that, for larger Γ than $3.86T_c$, the suppression of the Landau damping overwhelms the increase of the quasiparticles by the depairing effect, and the CG mode appears in $S(\mathbf{q},\omega)$ even in d-wave superconductors. However, since the d-wave superconductivity is absent for $\Gamma \geqslant 1.76T_c^0$ and $\Gamma=3.86T_c$ corresponds to $\Gamma=1.4T_c^0$ (namely, the superconductivity is almost suppressed), this possibility seems difficult.
[31] H. A. Fertig and S. D. Sarma, Phys. Rev. B **44**, 4480 (1991).
[32] M. Tachiki, T. Koyama, and S. Takahashi, Phys. Rev. B **50**, 7065 (1994).
[33] Y. Ohashi and S. Takada, Phys. Rev. B **59**, 4404 (1999).
[34] Y. Ohashi and S. Takada, Phys. Rev. B **61**, 4276 (2000).
[35] T. Koyama, J. Phys. Soc. Jpn. **68**, 2010 (1999).
[36] K. Tamasaku, Y. Nakamura, and S. Uchida, Phys. Rev. Lett. **69**, 1455 (1992).
[37] Ophelia K. C. Tsui, N. P. Ong, Y. Matsuda, Y. F. Yan, and J. B. Peterson, Phys. Rev. Lett. **73**, 724 (1994).
[38] Y. Matsuda, M. B. Gaifullin, K. Kumagai, K. Kadowaki, and T. Mochiku, Phys. Rev. Lett. **75**, 4512 (1995).
[39] K. Kadowaki, I. Kakeya, M. B. Gaifullin, T. Mochiku, S. Takahashi, T. Koyama, and M. Tachiki, Phys. Rev. B **56**, 5617 (1997).
[40] M. B. Gaifullin, Y. Matsuda, and L. N. Bulaevski, Phys. Rev. Lett. **81**, 3551 (1998).
[41] K. Kadowaki, I. Kakeya, T Wakabayashi, R. Nakamura, and S. Takahashi (unpublished).
[42] A. A. Tsvetkov, D. van der Marel, K. A. Moler, J. R. Kirtley, J. L. de Boer, A. Meetsma, Z. F. Ren, N. Koleshnikov, D. Dulic, A. Damascelli, M. Grüninger, J. Schützmann, J. W. van der Eb, H. S. Somal, and J. H. Wang, Nature (London) **395**, 360 (1998).
[43] M. B. Gaifullin, Y. Matsuda, N. Chikumoto, J. Shimoyama, K. Kishio, and R. Yoshizaki, Phys. Rev. Lett. **83**, 3928 (1999).